

Local circulations in and around the Ulaanbaatar, Mongolia, metropolitan area

Gantuya Ganbat¹ · Jong-Jin Baik¹

Received: 23 September 2014/Accepted: 18 March 2015
© Springer-Verlag Wien 2015

Abstract Many cities around the world are located in mountainous areas. Understanding local circulations in mountainous urban areas is important for improving local weather and air quality prediction as well as understanding thermally forced mesoscale flow dynamics. In this study, we examine local circulations in and around the Ulaanbaatar, Mongolia, metropolitan area using the Weather Research and Forecasting model coupled with the Seoul National University Urban Canopy Model. Ulaanbaatar lies in an east–west-oriented valley between the northern base of Mt. Bogd Khan and the southern base of branches of the Khentiin Nuruu mountain range. Idealized summertime fair-weather conditions with no synoptic winds are considered. In the daytime, mountain upslope winds, up-valley winds, and urban breeze circulation form and interact with each other. Mountain upslope winds precede up-valley winds. It is found that the transition of upslope winds to downslope winds on the urban-side slope of Mt. Bogd Khan occurs and the downslope winds in the afternoon strengthen due to urban breezes. In the nighttime, mountain downslope winds and down-valley winds are prominent and strong channeling flows form over the city. The sensitivities of local circulations to urban fraction, atmospheric stability, and soil water content are examined. As urban fraction increases, daytime up-valley winds over the city and daytime downslope winds on the urban-side slope of Mt. Bogd Khan strengthen. Daytime near-surface up-

valley winds in the city strengthen with increasing atmospheric stability. As soil water content decreases, daytime near-surface up-valley winds in the city weaken. The daytime urban atmospheric boundary-layer height is found to be sensitive to atmospheric stability and soil water content. This study is a first attempt to examine local circulations in and around the Ulaanbaatar metropolitan area and demonstrates that the city alters mountain slope winds and up-/down-valley winds.

1 Introduction

Local circulations/winds, such as sea/land breeze circulation, urban breeze circulation, mountain/valley winds, and up-/down-valley winds, are thermally forced flows, which are well developed under clear skies and with weak synoptic winds. Larger surface sensible heat flux in urban areas than in surrounding rural areas results in circulation called the urban heat island circulation or urban breeze circulation. Many observational and numerical modeling studies have been performed to better understand the urban breeze circulation (e.g., Lemonsu and Masson 2002; Hidalgo et al. 2008a, b; Miao et al. 2009; Ryu and Baik 2013).

The urban breeze circulation can be affected by mountain slope winds and/or valley winds if a city is located in/near a mountainous area. Previous numerical modeling studies have demonstrated that the urban breeze circulation counteracts mountain upslope winds in the daytime while the urban breeze circulation enhances mountain downslope winds in the nighttime (e.g., Lee and Kim 2010; Ryu and Baik 2013; Ganbat et al. 2015). Giovannini et al. (2014) examined boundary-layer processes and urban-induced alterations in an Alpine valley and showed that valley winds

Responsible Editor: S. Hong.

✉ Jong-Jin Baik
jjbaik@snu.ac.kr

¹ School of Earth and Environmental Sciences, Seoul National University, Seoul 151-742, South Korea

are effectively altered due to the presence of Trento city, Italy. Ganbat et al. (2015) examined the interactions of urban breeze circulation with mountain slope winds. They showed that the extent of the interactions between urban breeze circulation and mountain slope winds depends on urban fraction and mountain height.

Many factors affect local circulations in mountainous urban areas, including urban fraction, atmospheric boundary-layer stability, and soil water content. Urban fraction is an important factor that determines the amount of surface sensible heat flux in the urban area which is associated with the intensity of urban breeze circulation. The stability of the atmospheric boundary layer greatly affects the urban heat island circulation (e.g., Vukovich and Dunn 1978; Richiardone and Brusasca 1989; Baik et al. 2007). Baik et al. (2007) numerically and theoretically investigated the effects of atmospheric boundary-layer stability on the urban heat island circulation, showing that the boundary-layer flow becomes strong as atmospheric boundary-layer stability decreases. Through idealized numerical simulations, Martilli (2003) showed that the daytime urban atmospheric boundary layer is very sensitive to rural soil water content.

This study aims to numerically investigate local circulations in and around the Ulaanbaatar, Mongolia, metropolitan area using a mesoscale model. Ulaanbaatar is located at an elevation of ~ 1350 m and in complex terrain. Idealized numerical simulations under clear skies and with no synoptic winds are considered. Sensitivity experiments are conducted to examine the sensitivities of local circulations to urban fraction, atmospheric stability, and soil water content. In Sect. 2, numerical model and experimental settings are described. Simulation results are presented and discussed in Sect. 3. Section 4 includes a summary and conclusions.

2 Numerical model and experimental settings

The Weather Research and Forecasting (WRF) model version 3.2 (Skamarock et al. 2008) coupled with the Seoul National University Urban Canopy Model (SNUUCM) (Ryu et al. 2011) is used in this study. Selected physical parameterization schemes include the Dudhia shortwave radiation scheme (Dudhia 1989), the Rapid Radiative Transfer Model (RRTM) longwave radiation scheme (Mlawer et al. 1997), the Yonsei University (YSU) planetary boundary layer scheme (Hong et al. 2006), and the Purdue Lin cloud microphysics scheme (Lin et al. 1983). The SNUUCM developed by Ryu et al. (2011) parameterizes the essential physical processes that occur in urban canopies including absorption and reflection of shortwave and longwave radiation, exchanges of turbulent

energy and water between surfaces (road, two facing walls, and roof) and adjacent air, and heat transfer by conduction through substrates. The SNUUCM is coupled with the Noah land surface model (Chen and Dudhia 2001) using a tile approach. The topographic shadow effect is not considered in this study.

The computational domain size is $215 \text{ km} \times 215 \text{ km}$ in the horizontal with a horizontal grid resolution of 500 m. The regions with outermost 30 grids are buffer regions, where the terrain height is gradually reduced from the lateral boundaries of the physical domain ($200 \text{ km} \times 200 \text{ km}$) (Fig. 1a) to reduce steepness at/near the lateral boundaries. The model top height is 8 km. The number of vertical layers is 83, and the lowest model level is ~ 20 m. The initial temperature at the surface is 20°C , and the initial wind is calm. The lateral boundary condition is periodic. The Earth's rotation is included. In the control

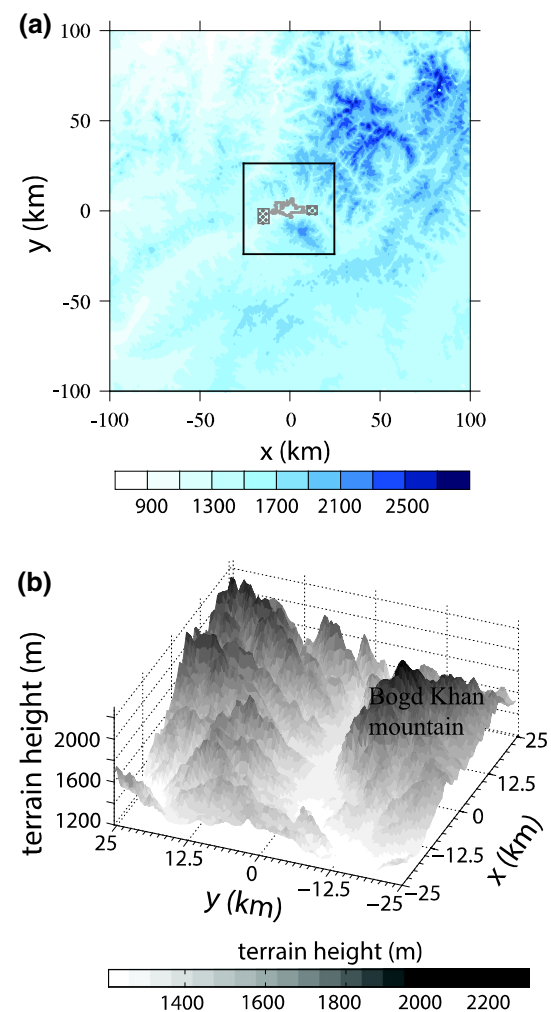
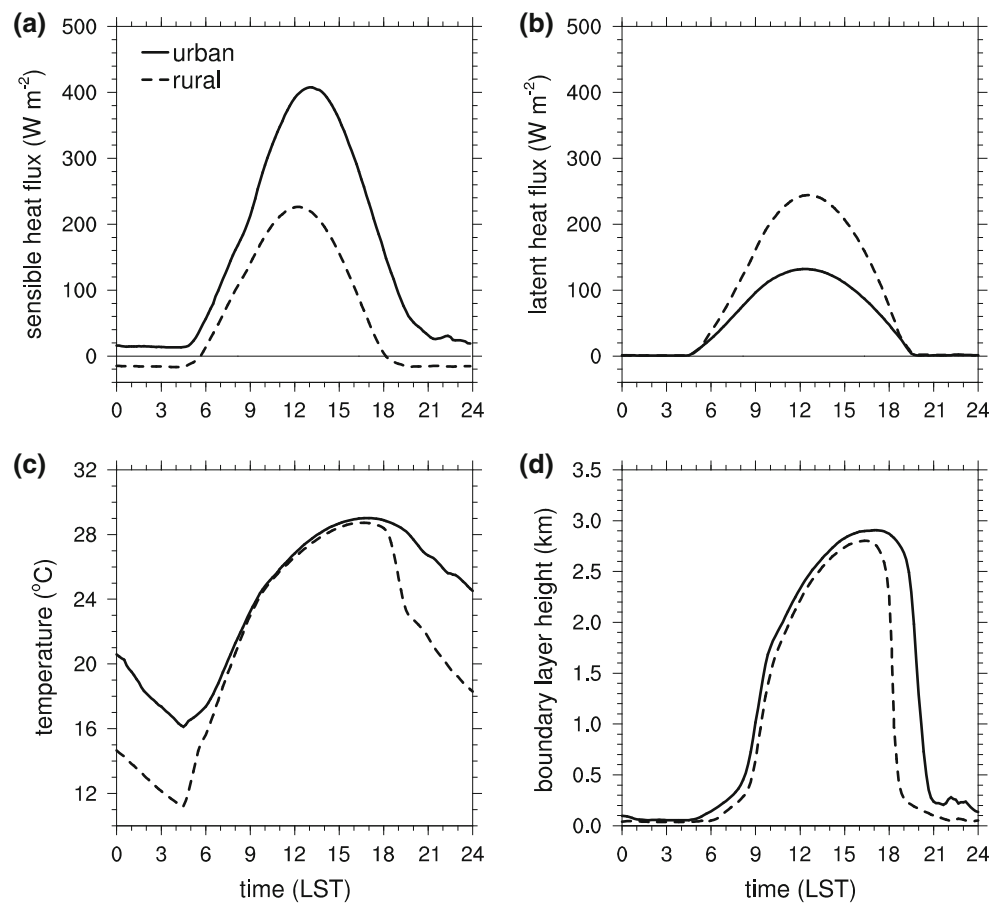


Fig. 1 Terrain height in the **a** physical and **b** analysis domains. The inner rectangle in **a** is the analysis domain. The urban boundary is indicated by gray line in **a**, and dotted boxes in **a** indicate the rural analysis areas

Fig. 2 Diurnal variations of **a** surface sensible heat flux, **b** surface latent heat flux, **c** air temperature at 2 m, and **d** atmospheric boundary-layer height averaged over the urban and rural areas in the control simulation



simulation, the initial potential temperature lapse rate is 5 K km^{-1} , the initial relative humidity is 30 %, and the initial volumetric soil water content is $0.17 \text{ m}^3 \text{ m}^{-3}$. The model is integrated for 36 h starting from 1200 LST July 14, 2013, with a time step of 1 s. Here, the year has no meaning.

The urban grid consists of built-up (70 %) and natural (30 %) areas. These are values for Ulaanbaatar. All natural areas consist of grassland (52.5 %) and bare ground with sandy loam soil (47.5 %). The value of 52.5 % is based on the observation. Some important urban parameters in the SNUUCM are specified as follows. The roof level height is 10 m, and the aspect ratio is 0.5. These are values for Ulaanbaatar. The albedos of roof, wall, and road are 0.12, 0.12, and 0.08, respectively (Ryu et al. 2013). The anthropogenic heat for Ulaanbaatar is considered in this study. The anthropogenic heat varies diurnally with its maximum value of 20 W m^{-2} and its minimum value of 9 W m^{-2} .

Topography in the study area is complex. Ulaanbaatar lies in a nearly east–west-oriented valley between the southern base of branches of the Khentiin Nuruu mountain range (with a maximum height of approximately 2800 m) and the northern base of Mt. Bogd Khan (with a maximum

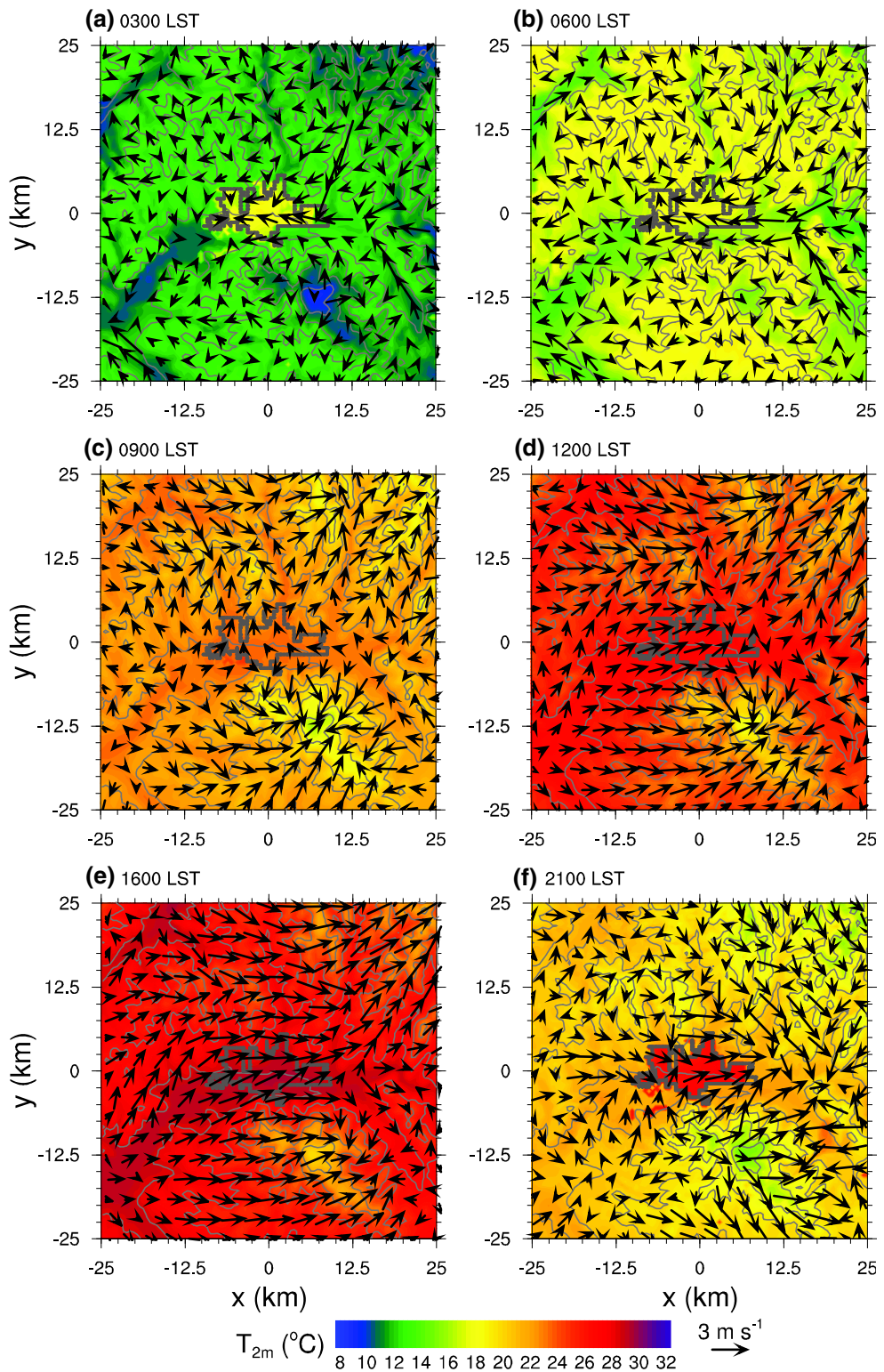
height of approximately 2200 m) (Fig. 1). The valley terrain height decreases from east (valley mouth) to west (valley exit). The valley exit is connected to a wide basin. Several tributaries join in the valley. Figure 1b shows the topographic features of the area with a size of $50 \text{ km} \times 50 \text{ km}$ centered on Ulaanbaatar which is taken for the analysis in this study (hereafter, analysis domain). The Shuttle Radar Topography Mission (SRTM) data with a resolution of $\sim 90 \text{ m}$ (Jarvis et al. 2008) are utilized for terrain data in this study. The United States Geological Survey (USGS) dataset and a combined dataset for Ulaanbaatar which includes the Moderate Resolution Imaging Spectroradiometer (MODIS) data (Friedl et al. 2002), a GlobCover land cover classifications map (Arino et al. 2010), and Google Earth imagery (Google Inc. 2013) are utilized for land-use/land-cover data.

3 Results and discussion

3.1 Control simulation

Figure 2 shows the diurnal variations of surface sensible heat flux, surface latent heat flux, 2-m air temperature, and

Fig. 3 Fields of air temperature at 2 m and wind vector at 10 m at **a** 0300, **b** 0600, **c** 0900, **d** 1200, **e** 1600, and **f** 2100 LST in the control simulation. The dark gray line indicates the urban boundary. Light gray lines indicate the terrain height (from 1300 to 2100 m with intervals of 200 m)



atmospheric boundary-layer height averaged over the urban area (the gray line in Fig. 1a indicates the urban boundary) and rural areas (dotted boxes in Fig. 1a). Here, the rural areas, which have size and terrain height similar to

those in the urban area, are chosen on the valley mouth and exit. In the daytime, the surface sensible heat flux is larger in the urban area than in the rural areas while the surface latent heat flux is smaller in the urban area than in the rural

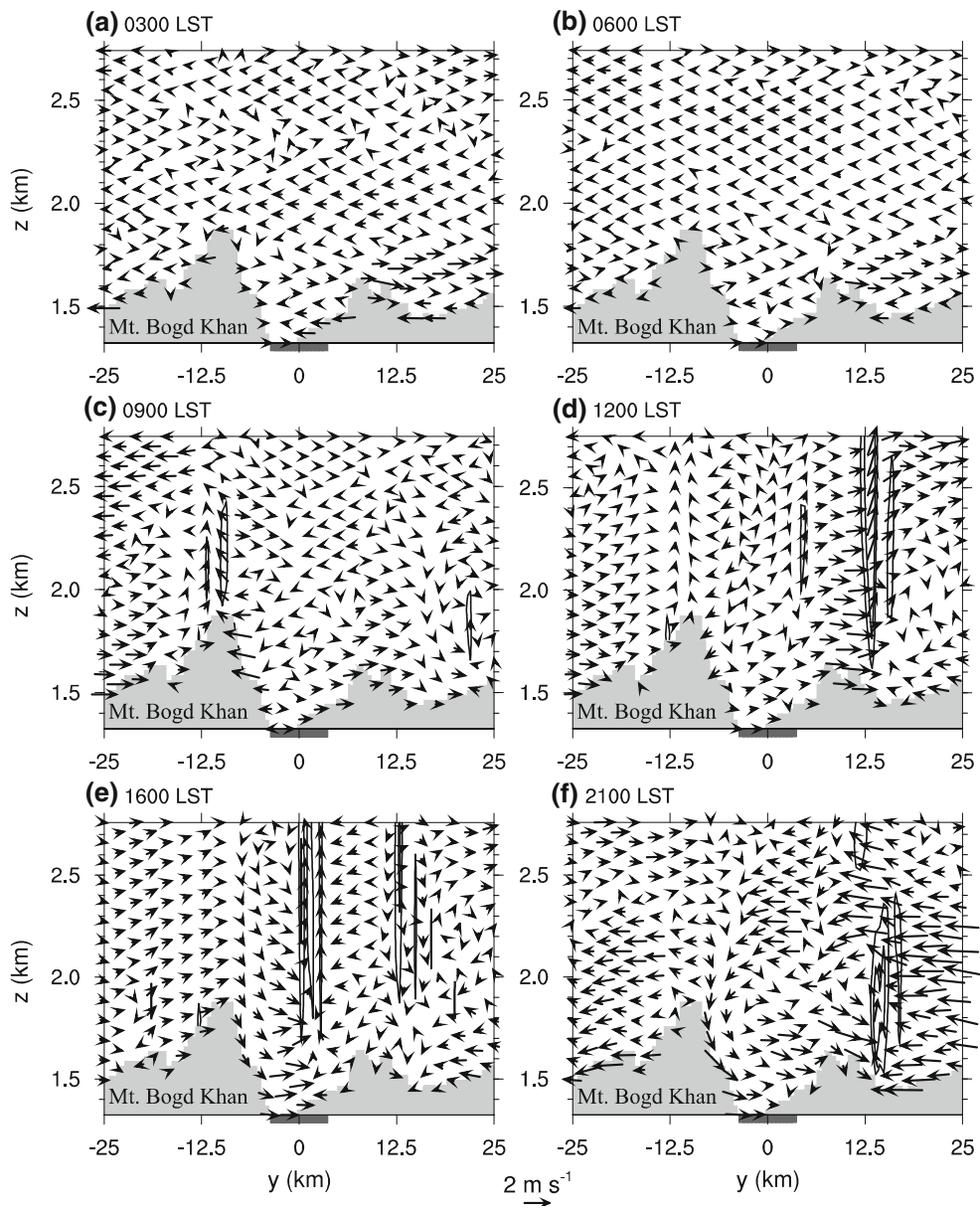


Fig. 4 Vertical cross-sections of wind vector and vertical velocity (contours) along the south-north direction through the center of the analysis domain at **a** 0300, **b** 0600, **c** 0900, **d** 1200, **e** 1600, and **f** 2100

LST in the control simulation. The contour levels of vertical velocity are 0.5 and 1 m s^{-1} . The dark gray bar on the horizontal axis indicates the urban area

areas. This finding is consistent with the results of previous studies (e.g., Hidalgo et al. 2008b; Lee and Baik 2011). In the urban area, the maximum surface sensible heat flux is 408 W m^{-2} at 1300 LST and the maximum surface latent heat flux is 132 W m^{-2} at 1220 LST. The larger daytime surface sensible heat flux in the urban area results in deeper daytime atmospheric boundary layer. The difference in 2-m air temperature between the urban and rural areas, which represents the urban heat island, is large in the nighttime and very small in the daytime. This feature of the simulated urban heat island is similar to that of the observed one in Ulaanbaatar (Ganbat et al. 2013). The maximum urban heat

island intensity is 5.0°C at 0350 LST. The atmospheric boundary-layer height in the urban area (rural areas) reaches a maximum of 2906 (2802) m at 1710 (1620) LST. The simulated atmospheric boundary layer is quite deep. A few studies have reported that the atmospheric boundary layer can exceed a depth of 3 km above the surface in the arid region (Ma et al. 2011) and over the Tibetan Plateau (Chen et al. 2013).

Previous studies showed that values of convective boundary layer depth calculated using the turbulent kinetic energy-based planetary boundary layer schemes are smaller than the observed while the values of convective

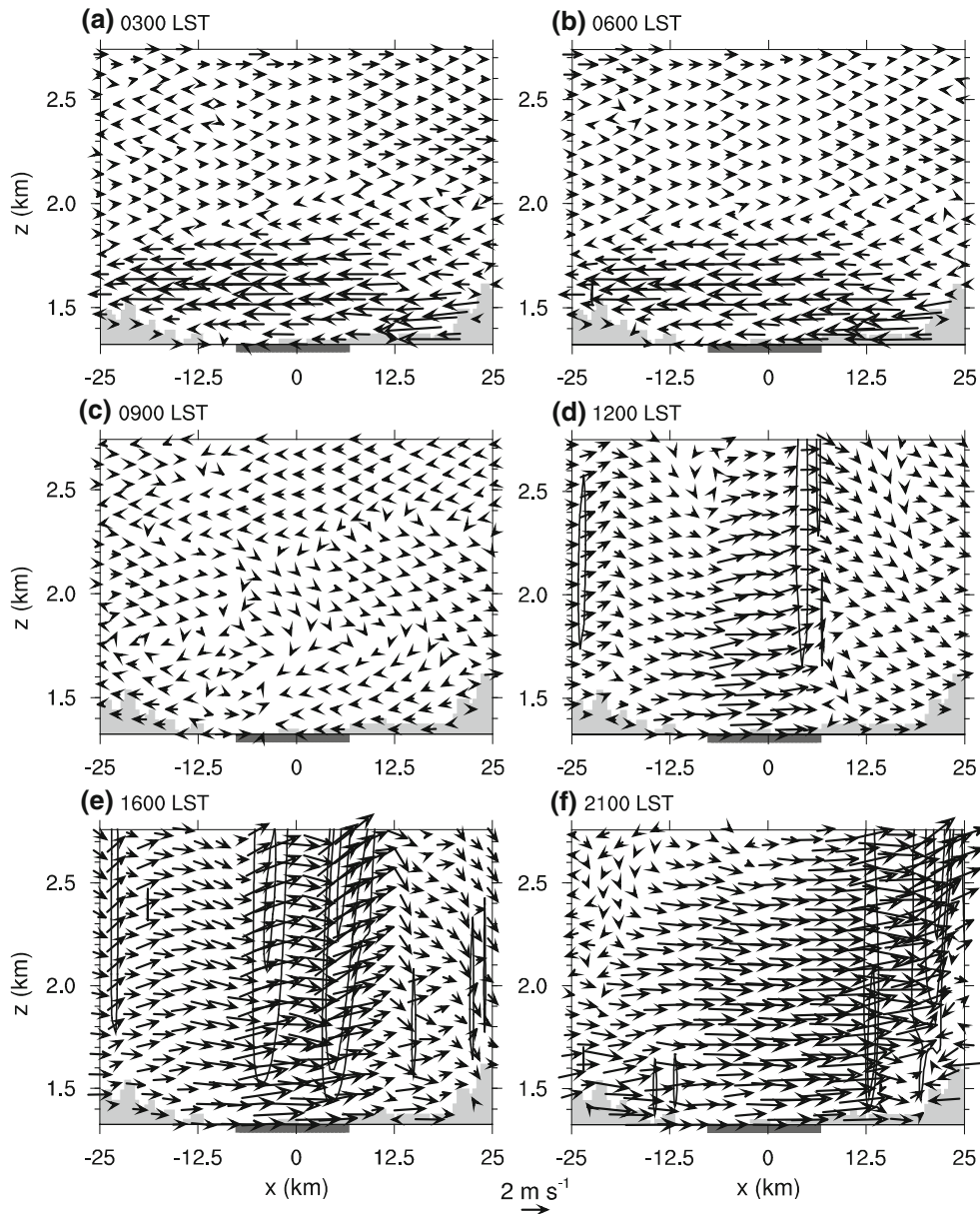


Fig. 5 Same as in Fig. 4 but for the east–west direction. The contour levels of vertical velocity are 0.5, 1, and 2 m s^{-1}

boundary layer depth calculated using the YSU planetary boundary layer scheme are close or larger than the observed (e.g., LeMone et al. 2013). The sensitivity of convective boundary layer depth and also local circulations in and around the Ulaanbaatar metropolitan area to planetary boundary layer schemes deserves an investigation.

Local circulations and their interactions are investigated through the analysis of wind fields. Figure 3 shows 2-m air temperature and 10-m wind vector fields at 0300, 0600, 0900, 1200, 1600, and 2100 LST. Figure 4 shows the vertical cross-sections of wind vector and vertical velocity along the south–north direction through the center of the analysis domain ($x = 0 \text{ km}$, $y = 0 \text{ km}$) at the times

corresponding to Fig. 3. Figure 5 is the same as in Fig. 4 but for the east–west direction. It is mentioned that if the terrain is flat, only urban breeze circulation forms and mountain slope winds and up-/down-valley winds do not occur and that the urban breeze circulation is stronger in the daytime than in the nighttime. Note that the urban breeze circulation is featured by inward flow toward the center of a city in the lower atmospheric boundary layer, upward flow over the city, outward flow toward the surroundings in the upper atmospheric boundary layer, and downward flow in the surroundings (Hidalgo et al. 2010; Ryu et al. 2013). In the presence of the terrain, urban breeze circulation, mountain slope winds, and up-/down-

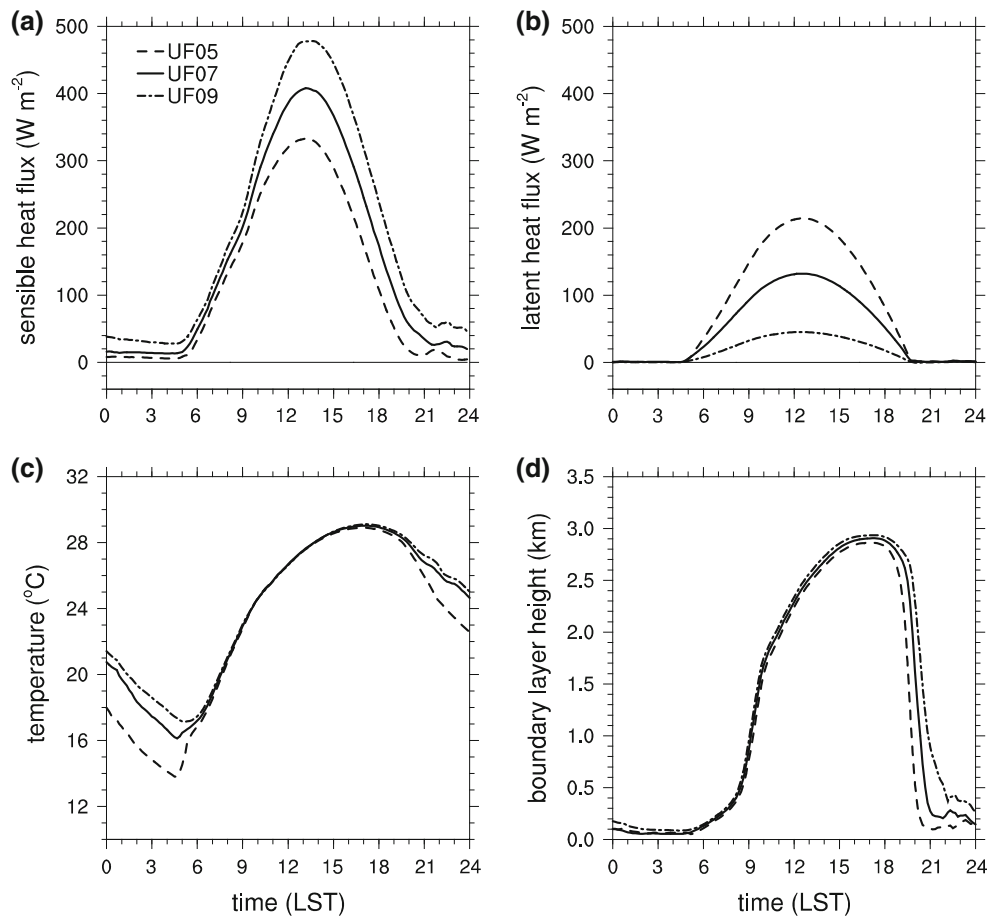


Fig. 6 Diurnal variations of **a** surface sensible heat flux, **b** surface latent heat flux, **c** air temperature at 2 m, and **d** atmospheric boundary-layer height averaged over the urban area in the UF05 (dashed), UF07 (solid), and UF09 (dot-dashed) simulations

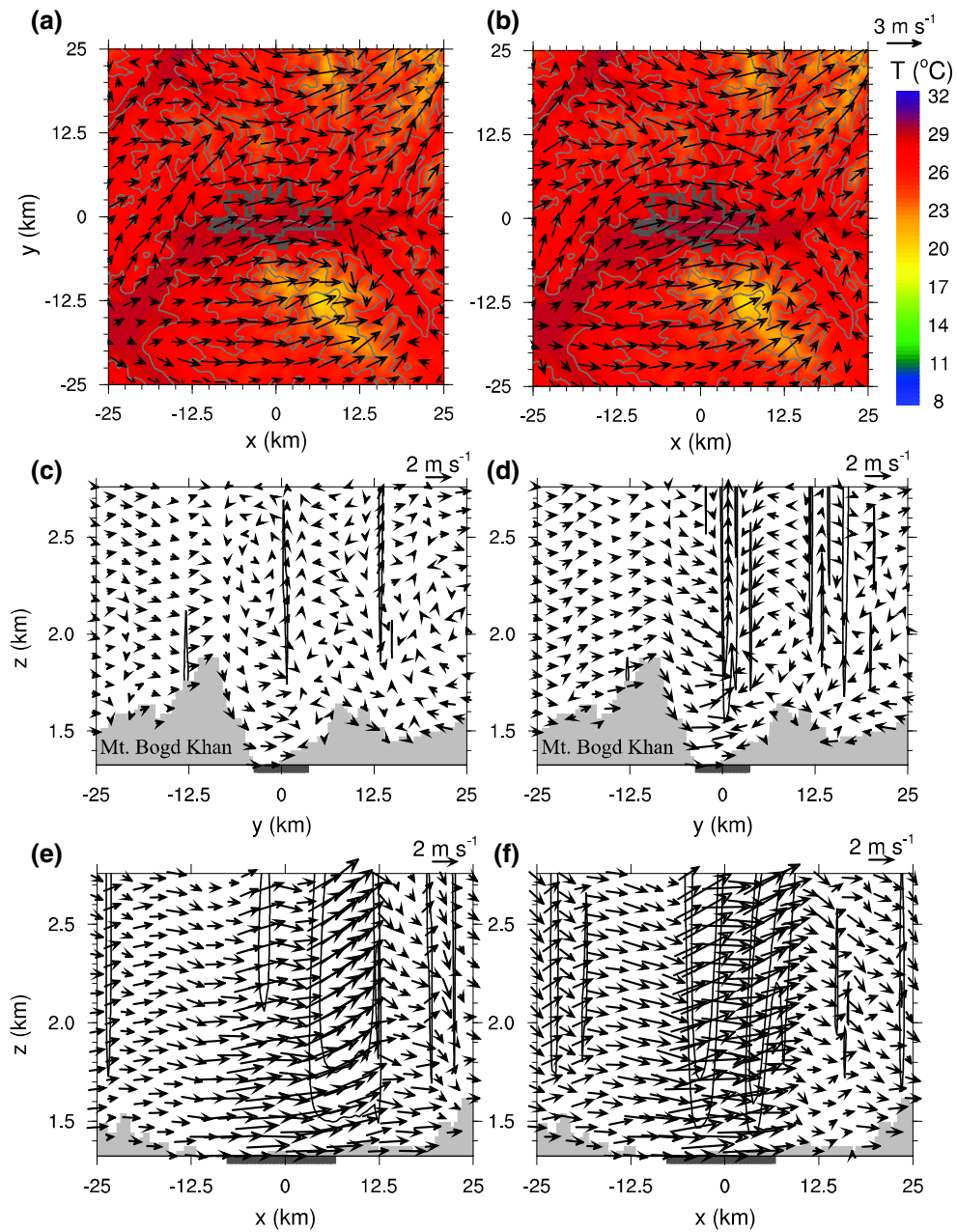
valley winds are produced and interact with each other. The simulated winds result from these interactions.

At 0300 LST, the air temperature in Ulaanbaatar is much higher than that in its surrounding areas, exhibiting a well-developed urban heat island, and down-valley winds in the city (easterly) and weak mountain downslope winds form (Fig. 3a). Down-valley winds are strong in some valley regions (e.g., valleys located to the northeast and southeast of Ulaanbaatar). Winds blowing from the tributary valleys join in/near the city valley. It is interesting to observe that down-valley winds in the city strengthen on the eastern side of the city. This is partially due to nighttime urban breezes. Down-valley winds over the city are prominent up to a height of ~ 600 m above the surface, featuring channeling flows (Fig. 5a). These results are largely consistent with those of Giovannini et al. (2014) which indicate that in the nighttime strong down-valley winds or channeling flows form over a valley city, Trento, and the city strengthens down-valley winds.

After sunrise, the near-surface air temperature gradually increases as the surface is heated by solar radiation. At

0600 LST, the air temperature difference between Ulaanbaatar and the surrounding areas is small and air temperatures are higher on mountain slopes than in valleys (Fig. 3b). Down-valley winds are still strong (Fig. 3b). In some regions, mountain upslope winds begin to develop (Figs. 3b, 4b). At 0900 LST, the urban heat island nearly disappears (Fig. 3c). Mountain upslope winds are well developed at this time (Fig. 3c), and updrafts are produced over the peak of Mt. Bogd Khan (Fig. 4c). Strong down-valley winds present at 0300 and 0600 LST disappear at 0900 LST (Fig. 3a–c). Along-valley winds at 0900 LST are very weak (Fig. 5c). At 1200 LST, mountain upslope winds are well developed and up-valley winds form (Fig. 3d). Up-valley winds over the city are found up to a height of ~ 1400 m above the surface (Fig. 5d). Moreover, up-valley winds near the valley mouth region of the valley city weaken due to urban breeze circulation (Figs. 3d, 5d). Based on Fig. 3b–d, mountain upslope winds precede up-valley winds. In the study area, the slope angle in the mountain slope regions is larger than that in the valley regions, leading to greater differential heating over the

Fig. 7 Fields of air temperature at 2 m and wind vector at 10 m in the **a** UF05 and **b** UF09 simulations and the vertical cross-sections of wind vector and vertical velocity (*contours*) along the south–north direction through the center of the analysis domain in the **c** UF05 and **d** UF09 simulations and along the east–west direction through the center of the analysis domain in the **e** UF05 and **f** UF09 simulations at 1600 LST. The dark gray line in **a** and **b** indicates the urban boundary. Light gray contours in **a** and **b** indicate the terrain height (from 1300 to 2100 m with intervals of 200 m). The dark gray bar on the horizontal axis in **c–f** indicates the urban area. The contour levels of vertical velocity in **c–f** are 0.5 and 1 m s^{-1}



mountain slopes than over the valleys. This explains to large extent why mountain upslope winds precede up-valley winds. At 1600 LST, mountain upslope winds and up-valley winds are well defined (Fig. 3e). Over the city, there are two regions with strong and relatively wide updrafts centered at $x = -3.5$ and 6 km (Fig. 5e). At 2100 LST, the urban heat island is established and local circulations are featured by up-valley winds in the city and mountain downslope winds (Fig. 3f).

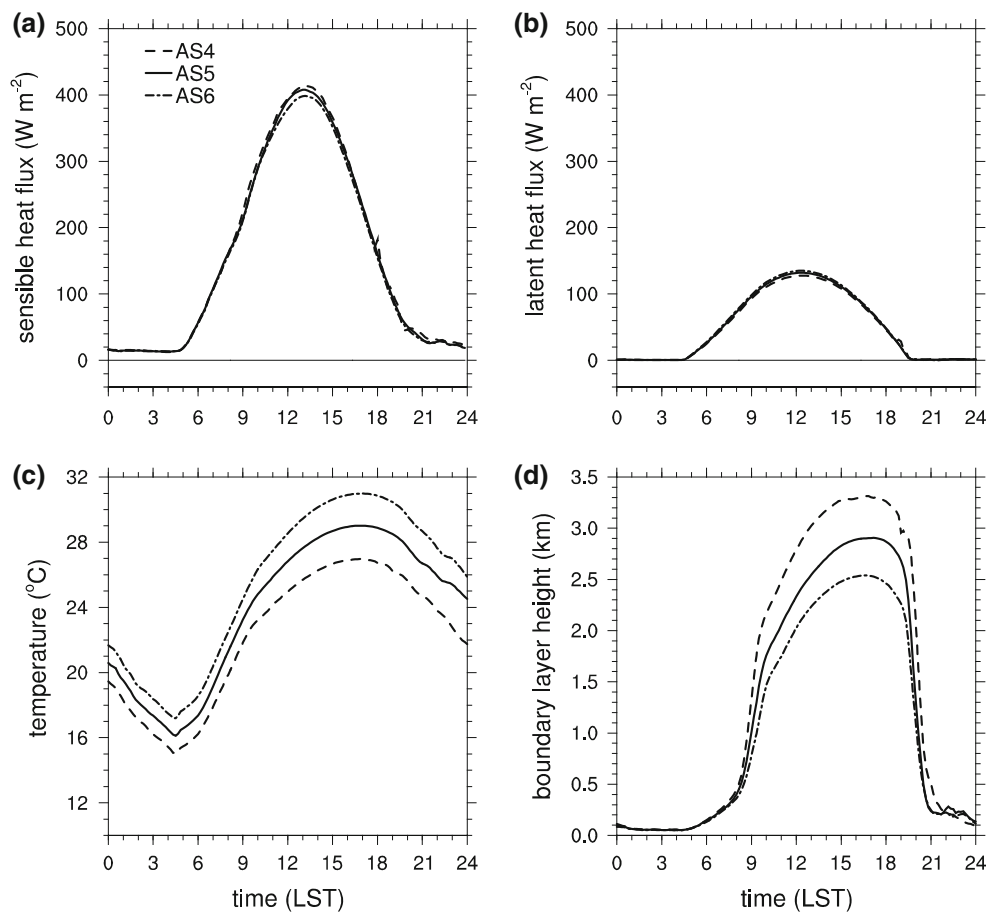
In the morning, upslope winds are developed on the urban-side (northern) slope of Mt. Bogd Khan (Fig. 4c). As the urban breeze circulation becomes strong, the upslope winds weaken and eventually become downslope winds

due to opposing urban breezes. Downslope winds on the urban-side slope of Mt. Bogd Khan are distinct in the late afternoon when the urban breeze circulation is strong (Fig. 4e). These features result from the interactions of urban breeze circulation with mountain slope winds. This finding agrees with the results of previous studies (e.g., Ganbat et al. 2015).

3.2 Sensitivity experiments

The sensitivity experiment results are presented and discussed in this subsection. The sensitivity of local circulations to urban fraction is examined by comparing

Fig. 8 Same as in Fig. 6 but for the AS4 (dashed), AS5 (solid), and AS6 (dot-dashed) simulations



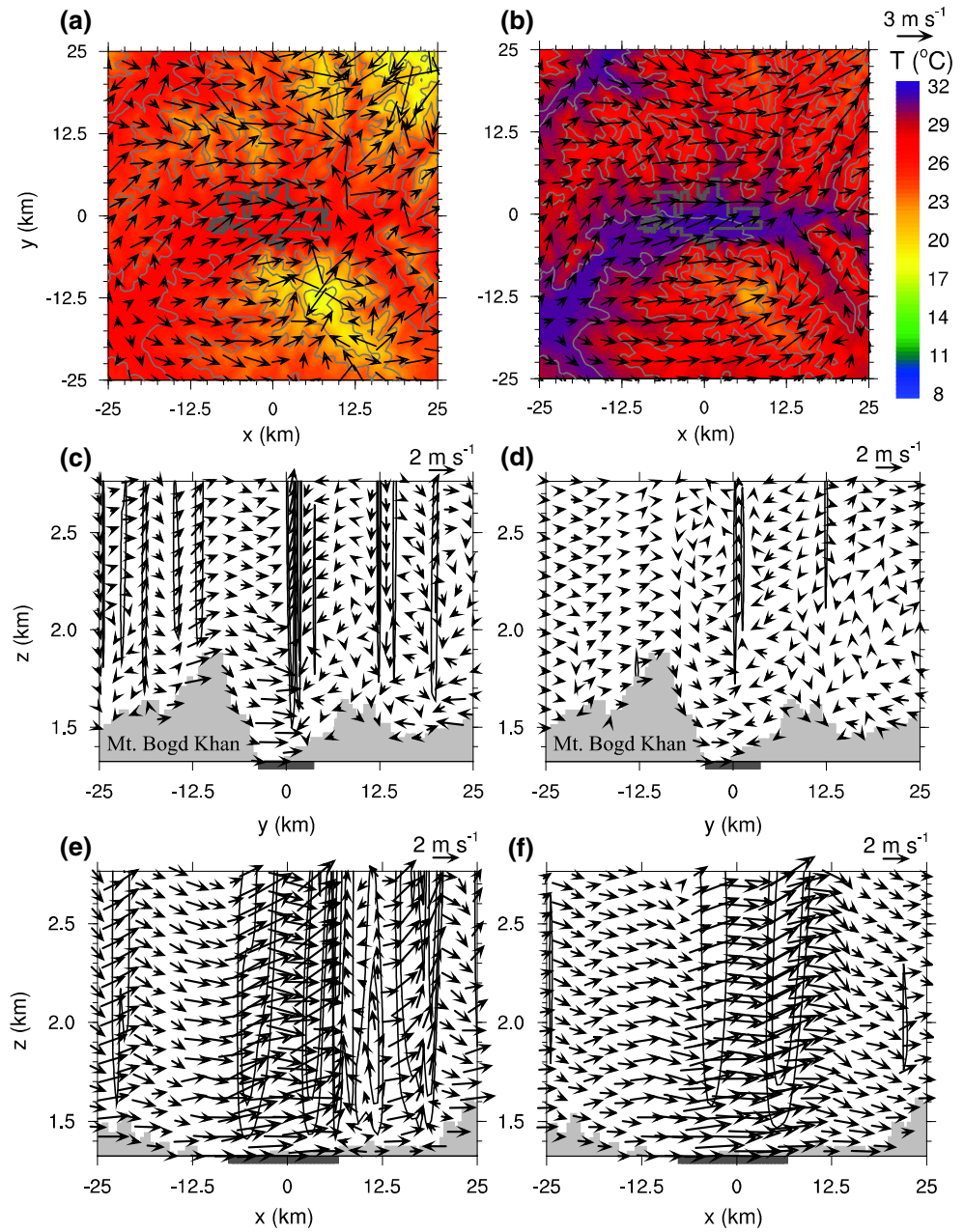
simulations with different urban fractions: 0.5 (simulation called UF05), 0.7 (UF07, control simulation), and 0.9 (UF09). The sensitivity of local circulations to atmospheric stability is examined by comparing simulations with different atmospheric stabilities: the initial potential temperature lapse rate is set to 4 (AS4), 5 (AS5, control simulation), and 6 (AS6) K km^{-1} . The sensitivity of local circulations to volumetric soil water content is examined by comparing simulations with different initial soil water contents: 0.09 (SW009), 0.17 (SW017, control simulation), and 0.25 (SW025) $\text{m}^3 \text{m}^{-3}$.

The diurnal variations of surface sensible heat flux, surface latent heat flux, 2-m air temperature, and atmospheric boundary-layer height averaged over the urban area in the UF05, UF07, and UF09 simulations are shown in Fig. 6. As expected, the UF09 simulation produces the largest daytime sensible heat flux and the smallest daytime latent heat flux. The urban area-averaged maximum sensible heat fluxes are 332, 408, and 478 W m^{-2} in the UF05, UF07, and UF09 simulations, respectively. The urban area-averaged maximum latent heat fluxes are 214, 132, and 45 W m^{-2} in the UF05, UF07, and UF09 simulations, respectively. In the nighttime, differences in 2-m air temperature between the UF09 and UF07 simulations are small

compared to those between the UF07 and UF05 simulations. The daytime 2-m air temperatures are very similar in the three simulations. Differences in atmospheric boundary-layer height between the simulations at any time are small except in the late afternoon/evening. The daytime maximum atmospheric boundary-layer height slightly increases as urban fraction increases.

Figure 7 shows 2-m air temperature and 10-m wind vector fields and the vertical cross-sections of wind vector and vertical velocity along the south-north and east-west directions through the center of the analysis domain at 1600 LST in the UF05 and UF09 simulations. For analysis, the time 1600 LST is selected in Fig. 7 (also, in Figs. 9, 11) because urban breeze circulation is well developed at this time so the interactions of daytime urban breeze circulation with other daytime local winds can be well revealed. The air temperature fields are similar to each other (Figs. 3e, 7a, b). The overall local circulation patterns are also similar to each other, but there are some differences in local circulation intensity. Downslope winds on the urban-side slope of Mt. Bogd Khan strengthen as urban fraction increases (Figs. 4e, 7c, d). This result is apparently due to strengthened urban breezes with increasing urban fraction. As urban fraction increases, up-valley winds over the city

Fig. 9 Same as in Fig. 7 but for the AS4 and AS6 simulations. The contour levels of vertical velocity in e–f are 0.5, 1, and 2 m s^{-1}



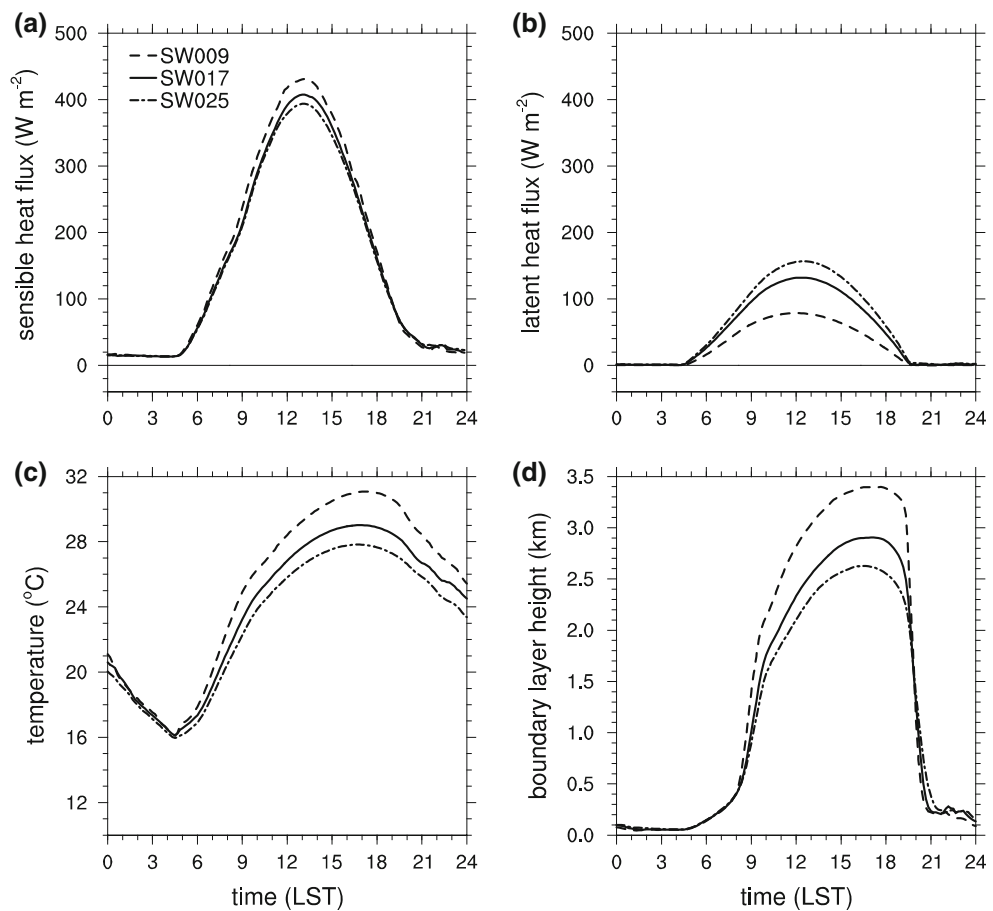
strengthen and up-valley winds near the valley mouth region of the valley city weaken (Figs. 5e, 7e, f). These features are also apparently due to strengthened urban breezes with increasing urban fraction.

Ulaanbaatar is the capital of Mongolia and is the highest populated administrative region in Mongolia. Ulaanbaatar has been rapidly urbanized in recent decades. The population of Ulaanbaatar increased from 0.8 million in 1999 to 1.3 million in 2013. The results of the sensitivity experiments of urban fraction imply that if urbanization continues, local winds in and near Ulaanbaatar will be altered. The alteration may include enhanced daytime up-

valley winds over the city and enhanced daytime down-slope winds on the urban-side slope of Mt. Bogd Khan.

The diurnal variations of surface sensible heat flux, surface latent heat flux, 2-m air temperature, and atmospheric boundary-layer height averaged over the urban area in the AS4, AS5, and AS6 simulations are shown in Fig. 8. Changes in atmospheric stability have insignificant impacts on surface sensible and latent heat fluxes but have significant impacts on air temperature and atmospheric boundary-layer height. As atmospheric stability increases, daytime and nighttime air temperatures increase and the daytime atmospheric boundary-layer height decreases. The

Fig. 10 Same as in Fig. 6 but for the SW009 (dashed), SW017 (solid), and SW025 (dot-dashed) simulations



urban area-averaged maximum atmospheric boundary-layer heights in the AS4, AS5, and AS6 simulations are 3313, 2906, and 2538 m, respectively.

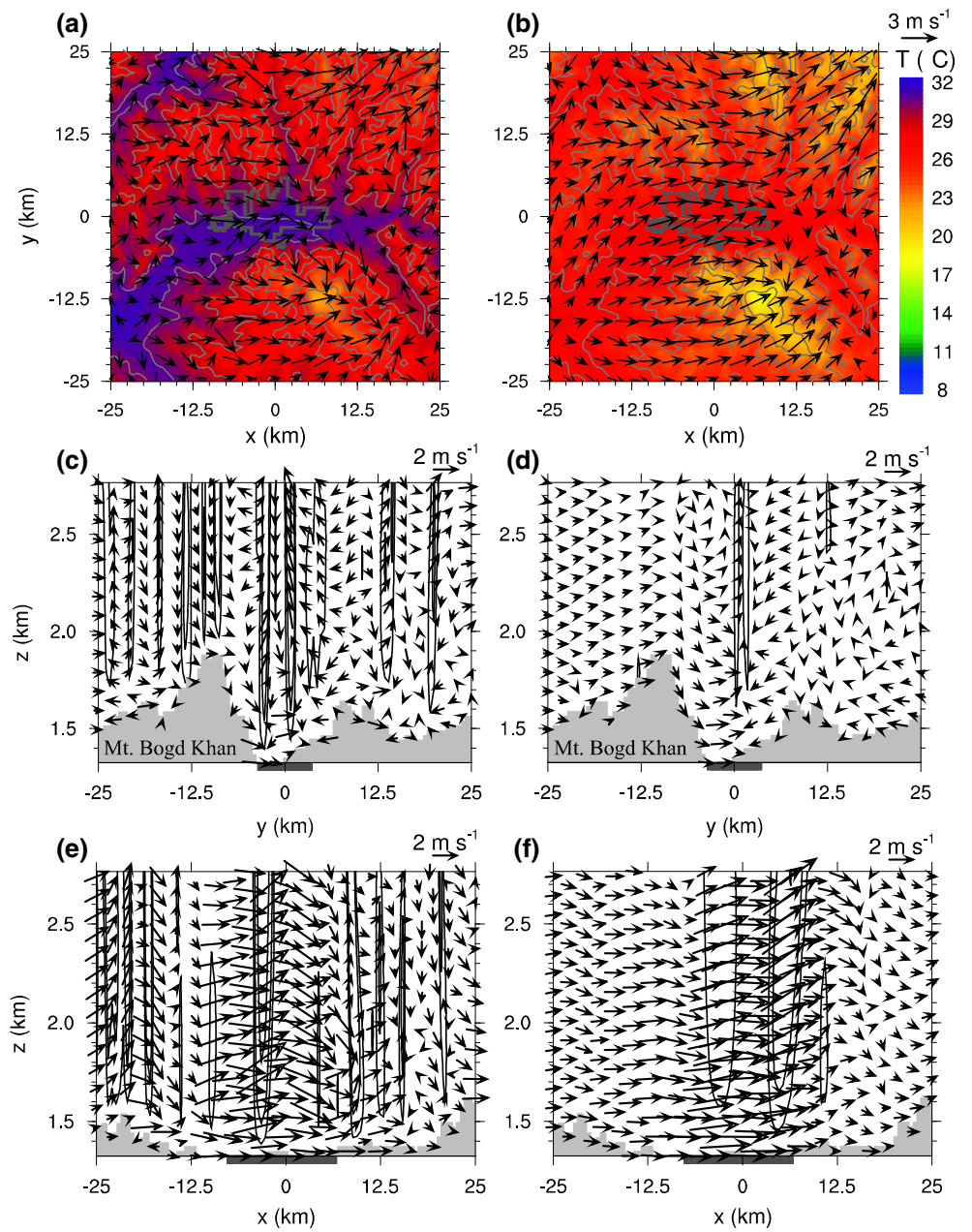
In this study, atmospheric stability means the stability of the atmosphere expressed in terms of the initial potential temperature lapse rate. Thus, atmospheric stability in this study can be roughly regarded as the basic-state atmospheric stability. Local circulations simulated in this study are largely confined to the lower atmosphere, i.e., within a few kilometers above the surface. In the simulations, the stability above the lower atmosphere changes very little with time, thus being similar to the basic-state atmospheric stability. However, the stability of the lower atmosphere varies with time, exhibiting convective boundary layers in the daytime in which the potential temperature is nearly constant with height and stable nighttime boundary layers. For larger atmospheric stability, more stable atmosphere above the lower atmosphere acts to suppress the growth of daytime convective boundary layer. This is a reason for less deep atmospheric boundary layer when atmospheric stability is larger (Fig. 8d).

Figure 9 shows 2-m air temperature and 10-m wind vector fields and the vertical cross-sections of wind vector

and vertical velocity along the south-north and east-west directions through the center of the analysis domain at 1600 LST in the AS4 and AS6 simulations. The air temperature field in the AS4 simulation exhibits cold regions at the higher altitudes of the mountains located to the northeast and southeast of Ulaanbaatar. In these regions, downslope winds are produced. In the AS6 simulation, air temperatures are high in the valleys. As atmospheric stability increases, up-valley winds become more consistently directed in the along-valley direction (Figs. 5e, 9e, f) and cross-valley winds tend to weaken (Figs. 4e, 9c, d). Near-surface up-valley winds strengthen with increasing atmospheric stability (Figs. 5e, 9e, f). This seems to be related to higher near-surface air temperature in the urban area for larger atmospheric stability.

The diurnal variations of surface sensible heat flux, surface latent heat flux, 2-m air temperature, and atmospheric boundary-layer height averaged over the urban area in the SW009, SW017, and SW025 simulations are shown in Fig. 10. As soil water content decreases, in the daytime the surface sensible heat flux increases, the surface latent heat flux decreases, and the air temperature increases. The diurnal air temperature range is the largest in the SW009

Fig. 11 Same as in Fig. 7 but for the SW009 and SW025 simulations. The contour levels of vertical velocity in c–f are 0.5, 1, and 2 m s^{-1}



simulation. The daytime atmospheric boundary-layer height is sensitive to soil water content. The urban area-averaged maximum atmospheric boundary-layer heights in the SW009, SW017, and SW025 simulations are 3397, 2906, and 2627 m, respectively.

Figure 11 shows 2-m air temperature and 10-m wind vector fields and the vertical cross-sections of wind vector and vertical velocity along the south-north and east–west directions through the center of the analysis domain at 1600 LST in the SW009 and SW025 simulations. As soil water content decreases, the air temperature increases (Figs. 3e, 11a, b). Based on the results of the atmospheric stability and soil water content sensitivity experiments, the

impact of drier soil on near-surface air temperature is similar to that of larger atmospheric stability on near-surface air temperature. For example, air temperatures are high in the valleys in both AS6 simulation (larger atmospheric stability) and SW009 simulation (drier soil) (Figs. 9b, 11a). In the SW009 simulation, numerous small-scale deep convective updraft cells form (Fig. 11c). As soil water content decreases, downslope winds on the urban-side upper slope of Mt. Bogd Khan weaken while downslope winds on the urban-side lower slope of Mt. Bogd Khan strengthen (Figs. 4e, 11c, d). As soil water content decreases, near-surface up-valley winds in the city weaken (Figs. 5e, 11c, d).

As soil becomes dry, that is, soil water content decreases, the daytime surface sensible heat flux increases. Note that the urban area consists of 30 % natural area. At 1600 LST, in the SW009 simulation the surface sensible heat flux averaged over the urban area is 321 W m^{-2} (19 W m^{-2} increase compared to the control simulation) and the surface sensible heat flux averaged over the rural areas is 155 W m^{-2} (49 W m^{-2} increase compared to the control simulation). Hence, the gradient in surface sensible heat flux between the urban and rural areas decreases, which leads to weaker urban breeze circulation and thereby weakened near-surface up-valley winds in the city.

4 Summary and conclusions

Local circulations in and around the Ulaanbaatar, Mongolia, metropolitan area were investigated for the first time through numerical simulations using a high-resolution mesoscale model coupled with the advanced urban canopy model (SNUUCM). Fair-weather conditions without the influence of synoptic-scale forcing were considered. In the daytime, local circulations are characterized by mountain upslope winds, up-valley winds, and urban breeze circulation. It was found that mountain upslope winds precede up-valley winds and that upslope winds change to downslope winds on the urban-side slope of Mt. Bogd Khan and the downslope winds in the afternoon strengthen due to urban breezes. In the nighttime, local circulations are characterized by mountain downslope winds and down-valley winds. Strong channeling flows form over the city. Local circulations were found to be sensitive to urban fraction, atmospheric stability, and soil water content. As urban fraction increases, daytime up-valley winds over the city and daytime downslope winds on the urban-side slope of Mt. Bogd Khan strengthen. As atmospheric stability increases, daytime up-valley winds become more consistently directed in the along-valley direction and daytime cross-valley winds tend to weaken. Near-surface up-valley winds in the city strengthen with increasing atmospheric stability. As soil water content decreases, downslope winds on the urban-side upper slope of Mt. Bogd Khan weaken while downslope winds on the urban-side lower slope of Mt. Bogd Khan strengthen. As soil water content decreases, daytime near-surface up-valley winds in the city weaken.

In this study, summertime local circulations in and around the Ulaanbaatar metropolitan area under clear skies and with no synoptic winds were investigated. Under these conditions, local circulations become well developed and their interactions are distinct. When synoptic winds are weak, the interactions of local circulations with large-scale winds (synoptic winds) can occur. The interactions can

differ depending on the large-scale wind direction. The interactions between local circulations and weak large-scale winds in the study area deserve an investigation. In winter, high-pressure systems dominate over the area, which produce persistent temperature inversion layers. Due to the presence of temperature inversion layers, Ulaanbaatar faces a severe air pollution problem in winter. An investigation of wintertime local circulations in the presence of a temperature inversion layer to address the air pollution problem is worthwhile.

Acknowledgments The authors are grateful to two anonymous reviewers for providing valuable comments on this work. This work was funded by the National Research Foundation of Korea (NRF) grant funded by the Korea Ministry of Science, ICT and Future Planning (MSIP) (No. 2012-0005674).

References

- Arino O, Ramos J, Kalogirou V, Defourny P, Achard F (2010) GlobCover 2009. In: Proceedings of ESA Living Planet Symposium, Bergen, Norway, ESA, SP-686
- Baik JJ, Kim YH, Kim JJ, Han JY (2007) Effects of boundary-layer stability on urban heat island-induced circulation. *Theor Appl Climatol* 89:73–81
- Chen F, Dudhia J (2001) Coupling an advanced land surface-hydrology model with the Penn State–NCAR MM5 modeling system. Part I: model implementation and sensitivity. *Mon Weather Rev* 129:569–585
- Chen X, Anel JA, Su A, de la Torre L, Kelder H, van Peet J, Ma Y (2013) The deep atmospheric boundary layer and its significance to the stratosphere and troposphere exchange over the Tibetan Plateau. *PLoS One* 8(2):e56909. doi:10.1371/journal.pone.0056909
- Dudhia J (1989) Numerical study of convection observed during the winter monsoon experiment using a mesoscale two-dimensional model. *J Atmos Sci* 46:3077–3107
- Friedl MA, McIver DK, Hodges JCF, Zhang XY, Muchoney D, Strahler AH, Woodcock CE, Gopal S, Schnieder A, Cooper A, Bacinni A, Gao F, Schaaf C (2002) Global land cover mapping from MODIS: algorithms and early results. *Remote Sens Environ* 83:287–302
- Ganbat G, Han JY, Ryu YH, Baik JJ (2013) Characteristics of the urban heat island in a high-altitude metropolitan city, Ulaanbaatar, Mongolia. *Asia Pac J Atmos Sci* 49:535–541
- Ganbat G, Baik JJ, Ryu YH (2015) A numerical study of the interactions of urban breeze circulation with mountain slope winds. *Theor Appl Climatol* 120:123–135
- Giovannini L, Zardi D, de Franceschi M, Chen F (2014) Numerical simulations of boundary-layer processes and urban-induced alterations in an Alpine valley. *Int J Climatol* 34:1111–1131
- Google Inc (2013) Google Earth. <http://maps.google.com>. Accessed 10 April 2013
- Hidalgo J, Masson V, Pigeon G (2008a) Urban-breeze circulation during the CAPITOUL experiment: numerical simulations. *Meteorol Atmos Phys* 102:243–262
- Hidalgo J, Pigeon G, Masson V (2008b) Urban-breeze circulation during the CAPITOUL experiment: observational data analysis approach. *Meteorol Atmos Phys* 102:223–241
- Hidalgo J, Masson V, Gimeno L (2010) Scaling the daytime urban heat island and urban breeze circulation. *J Appl Meteorol Climatol* 49:889–901

- Hong SY, Noh Y, Dudhia J (2006) A new vertical diffusion package with an explicit treatment of entrainment processes. *Mon Weather Rev* 134:2318–2341
- Jarvis A, Reuter HI, Nelson A, Guevara E (2008) Hole-filled SRTM for the globe version 4. <http://srtm.csi.cgiar.org>. Accessed 28 Jan 2011
- Lee SH, Baik JJ (2011) Evaluation of the vegetated urban canopy model (VUCM) and its impacts on urban boundary layer simulation. *Asia Pac J Atmos Sci* 47:151–165
- Lee SH, Kim HD (2010) Modification of nocturnal drainage flow due to urban surface heat flux. *Asia Pac J Atmos Sci* 46:453–465
- LeMone MA, Tewari M, Chen F, Dudhia J (2013) Objectively determined fair-weather CBL depths in the ARW-WRF model and their comparison to CASES-97 observations. *Mon Weather Rev* 141:30–54
- Lemonsu A, Masson V (2002) Simulation of a summer urban-breeze over Paris. *Bound Layer Meteorol* 104:463–490
- Lin YL, Farley RD, Orville HD (1983) Bulk parameterization of the snow field in a cloud model. *J Clim Appl Meteorol* 22:1065–1092
- Ma M, Pu Z, Wang S, Zhang Q (2011) Characteristics and numerical simulations of extremely large atmospheric boundary-layer heights over an arid region in north-west China. *Bound Layer Meteorol* 140:163–176
- Martilli A (2003) A two-dimensional numerical study of the impact of a city on atmospheric circulation and pollutant dispersion in a coastal environment. *Bound Layer Meteorol* 108:91–119
- Miao S, Chen F, LeMone MA, Tewari M, Li Q, Wang Y (2009) An observational and modeling study of characteristics of urban heat island and boundary layer structures in Beijing. *J Appl Meteorol Climatol* 48:484–501
- Mlawer EJ, Taubman SJ, Brown PD, Iacono MJ, Clough SA (1997) Radiative transfer for inhomogeneous atmospheres: RRTM, a validated correlated-k model for the longwave. *J Geophys Res* 102:16663–16682
- Richardson R, Brusasca G (1989) Numerical experiments on urban heat island intensity. *Quart J Roy Meteorol Soc* 115:983–995
- Ryu YH, Baik JJ (2013) Daytime local circulations and their interactions in the Seoul metropolitan area. *J Appl Meteorol Climatol* 52:784–801
- Ryu YH, Baik JJ, Lee SH (2011) A new single-layer urban canopy model for use in mesoscale atmospheric models. *J Appl Meteorol Climatol* 50:1773–1794
- Ryu YH, Baik JJ, Han JY (2013) Daytime urban breeze circulation and its interaction with convective cells. *Quart J Roy Meteorol Soc* 139:401–413
- Skamarock WC, Klemp JB, Dudhia J, Gill DO, Barker DM, Duda MG, Huang XY, Wang W, Powers JG (2008) A description of the advanced research WRF version 3. NCAR, Boulder
- Vukovich FM, Dunn JW (1978) A theoretical study of the St. Louis heat island: Some parameter variations. *J Appl Meteorol* 17:1585–1594